Catena 157 (2017) 333–343

Contents lists available at ScienceDirect

Catena

journal homepage: www.elsevier.com/locate/catena

Extrusive carbonatite outcrops – A source of chemical elements imbalance in topsoils of oceanic volcanic islands

R. Marques[a,*], M.I. Prudêncio[a], J.C. Waerenborgh[a], B.J.C. Vieira[a], F. Rocha[b,c], M.I. Dias[a], J. Madeira[d], J. Mata[d]

[a] Centro de Ciências e Tecnologias Nucleares (C2TN), Instituto Superior Técnico, Universidade de Lisboa, EN10 (139.7 km), 2695-066 Bobadela, Portugal
[b] GeoBioTec, Universidade de Aveiro, 3810-193 Aveiro, Portugal
[c] Dep. de Geociências, Universidade de Aveiro, 3810-193 Aveiro, Portugal
[d] Instituto Dom Luiz, Faculdade de Ciências, Universidade de Lisboa, 1749-016 Lisboa, Portugal

ARTICLE INFO

Keywords:
Extrusive carbonatite
Surficial layer of soil
Brava Island (Cape Verde)
REE
Trace elements
Iron speciation

ABSTRACT

Extrusive carbonatite ash tuff (Tantum) and spatter (Monte Miranda) deposits, and topsoils (incipient and shallow) from both sites of Brava Island (Cape Verde archipelago) were studied by neutron activation analysis, X-ray diffraction and Mössbauer spectroscopy. The ash tuff deposit near Tantum, here reported for the first time, corresponds to an extrusive calciocarbonatite with high W, Th, U and REE contents and a positive Eu anomaly. Similar REE patterns and W concentrations were also found in the spatter deposit of Monte Miranda. Magnetite is the major iron containing phase in both extrusive carbonatite deposits. High W and REE concentrations associated with the presence of calcite prevail in topsoils with extrusive carbonatite influence. In the topsoil developed on extrusive carbonatite ashes, magnetite is well preserved particularly in the coarser fractions probably due to the recent age of the parent material associated with the semi-arid climate of the island; a significant chemical heterogeneity of the whole samples as well as of the different size fractions of these topsoils was found, with an enrichment of Co, Zn, Ga, As, Br, Rb, Ce, and particularly Sb and W in the clay-size fraction, which may be relevant for the study of environmental health issues in Brava Island.

1. Introduction

Carbonatites are magmatic rocks with > 50% volume of carbonate minerals, characterized by high contents of Sr, Ba, P and light rare earth elements. They can be divided into calcio-, dolomitic- or magnesio-, ankeritic- and natro- carbonatites, according to the dominant carbonate mineral (e.g. Le Maitre, 2002). This type of rock usually occurs within stable, continental intraplate settings, more than half of them located in Africa (Jones et al., 2013). Their occurrence has been related to mantle plumes and large igneous provinces (Bell and Simonetti, 2010; Ernst and Bell, 2010). Intrusive types are dominant with volcanic outcrops representing only 10% of the known occurrences worldwide (Woolley and Church, 2005).

Oceanic carbonatites are extremely rare and their occurrence was first reported by Assunção et al. (1965) in Cape Verde, and by Fúster et al. (1968) and Allègre et al. (1971) in Fuerteventura (Canary Islands). However, Bebiano (1932) had already mentioned "calcareous dikes" and "calcareous masses of volcanic origin" in S. Vicente Island (Cape Verde). As far as we know, besides Cape Verde and Canary Islands no other occurrences of carbonatite outcrops in oceanic environments have been reported, although the occurrence of mantle metasomatism envolving carbonatite melts has been referred for Kerguelen (Mattielli et al., 2002) and Madeira Island (Mata et al., 1999).

In the Cape Verde islands calcio- to magnesio-carbonatites occur on 6 out of the 10 islands, and on the islets near Brava, and have been the subject of numerous studies (e.g., Allègre et al., 1971; De Ignacio et al., 2012; Doucelance et al., 2010; Jorgensen and Holm, 2002; Kogarko, 1993; Mata et al., 2010; Mourão et al., 2010, 2012a, 2012b). In this archipelago, intrusive carbonatites are clearly dominant, and several outcrops of this type of rock were mapped by Machado et al. (1968) within the basal complexes of several islands, while the first reference to extrusive carbonatite deposits was presented by Silva et al. (1981) in Santiago Island.

The occurrence of extrusive carbonatites in Brava Island was briefly mentioned in abstracts published by Tuberville et al. (1987) and Peterson et al. (1989). Later, Hoernle et al. (2002) described one occurrence at Cachaço in southern Brava. More recently, Mourão et al.

* Corresponding author.
E-mail address: rmarques@ctn.tecnico.ulisboa.pt (R. Marques).

http://dx.doi.org/10.1016/j.catena.2017.05.035
Received 7 February 2017; Received in revised form 22 May 2017; Accepted 30 May 2017

(2010) and Madeira et al. (2010) reported a more complete study of extrusive carbonatite outcrops corresponding to, at least, five eruptions and presenting a wide geographical dispersion on Brava Island. As reported by these authors, most of these extrusive carbonatitic formations are calciocarbonatites (according to the chemical systematics of Woolley and Kempe, 1989) and correspond to pyroclastic rocks, comprising magmatic and/or phreatomagmatic ash and lapilli fall deposits, and one pyroclastic flow. These carbonatitic eruptions are Quaternary in age and correspond to some of the younger volcanic events in Brava Island.

The semi-arid climate of Cape Verde archipelago and the rough topography of the landscape, with evidence of surface instability and recent erosion, originate incipient soils with low to moderate degree of weathering and development. The Geochemical Atlas of these islands using the chemical composition of topsoils (0–20 cm depth) is being done according to the recommendations of Darnley et al. (1995). Within this frame, a previous work performed on Brava topsoils (Marques et al., 2016) revealed that significant variations in chemical contents occur within the same geological unit, along with a chemical heterogeneity of the topsoils. High contents of Mn, Co, Ga, Ba, La, Ce, Nd, Sm, Eu, Tb, Ta, W, Th and U were observed in topsoils derived from carbonatites and phonolites; rare earth elements (REE) and W, as well as the predominance of low oxidized magnetite, appear to be good fingerprints for extrusive carbonatite outcrops. These features justify a deeper research of the previously identified topsoils by Marques et al. (2016) from Brava Island with extrusive carbonatite influence (5-BRV and 26-BRV samples). In this way further sampling of extrusive carbonatite outcrops near the identified topsoils was performed on: (a) one ash tuff deposit located at Tantum (reported for the first time in this work) and (b) the remains of a small hornito or spatter deposit near Monte Miranda (already referred by Mourão et al., 2010). A detailed compositional study was done by means of instrumental neutron activation analysis, Mössbauer spectroscopy and X-ray diffraction.

The specific objectives of the present work are: (a) the report of a newly found extrusive carbonatite outcrop near Tantum (Brava Island); and (b) the chemical and mineralogical characterization, and the iron speciation of extrusive carbonatites, and of different size fractions of the Tantum and Monte Miranda incipient topsoils (0-20 cm depth). This work is therefore a contribution for a more complete knowledge of: (i) rare oceanic extrusive carbonatite outcrops; (ii) the Brava extrusive carbonatites, which crop out in a wide geographical dispersion on the island; and (iii) the evaluation of the carbonatite influence on the imbalance of chemical elements in topsoils in the semi-arid environment of the Cape Verde archipelago.

2. Study area

Brava is a small semi-arid island (64 km^2) located on the south-western tip of the Cape Verde archipelago, in the NE–SW alignment formed together with Maio, Santiago and Fogo (Fig. 1). The exposed part of the island is formed by an older basement composed of the submarine volcanic edifice, comprising pillow lavas, pillow breccias and hyaloclastites of nephelinite/ankaramite composition, intruded by an alkaline-carbonatite complex, both of which are unconformably covered by younger sub-aerial volcanic deposits of dominant phonolitic composition (Madeira et al., 2010). These sequences led to the definition of three major volcano-stratigraphic units: (i) the older Lower Unit (2 to 3 Ma), composed of an uplifted seamount sequence representing the upper part of the submarine edifice precursor of island emergence; (ii) Middle Unit (1.8 to 1.3 Ma) corresponding to exhumed magma chambers forming a subvolcanic plutonic complex (including syenites, pyroxenites, ijolites and carbonatites), intruded into the Lower Unit; and (iii) Upper Unit (< 0.25 Ma), the younger volcanic sequence dominated by products of phonolite volcanism (characterized by phreatomagmatic and plinian pyroclastic deposits and by domes and lava flows) but also including small volumes of mafic (nephelinitic) and carbonatitic extrusions, standing on an important erosional discontinuity that truncates the older basement (Lower and Middle units) (Madeira et al., 2010; Mourão et al., 2010).

Extrusive carbonatites exposed within the Upper Unit constitute the focus of this contribution. At least 20 small outcrops of dark-brown to blackish extrusive carbonatites were found by Mourão et al. (2010) in three areas of Brava Island: in the NE around Nova Sintra, in the SW near Campo Baixo, and in the south around Cachaço and Morro das Pedras. All extrusive carbonatites were deposited at or near the top of the younger volcanic sequence. Most outcrops are made up of pyroclastic formations, comprising magmatic and/or phreatomagmatic ash and lapilli fall deposits, one pyroclastic flow, and a feeder dyke; most deposits contain abundant lithic fragments of phonolite and occasionally other lithologies.

3. Experimental

3.1. Sampling, materials and methods

Fieldwork was performed in 2013 in Brava Island, Cape Verde archipelago (see Fig.1), for the sampling of extrusive carbonatites outcrops and the surface layer of soil (0–20 cm depth), herein referred as topsoil. Field observations show an incipient pedogenesis of these shallow volcanic soils (≈ 30 cm depth).

Carbonatites were collected from two different sites: (a) near Tantum - a newly found outcrop of an ash fall deposit (5C–BRV) and the topsoil developed on it (5-BRV, Tantum topsoil) (UTM: X = 742,789 m, Y = 1,641,105 m), also with contribution of phonolite pyroclasts from the slope above, and (b) close to Monte Miranda (south of Cachaço) – a proximal spatter rampart (26R–BRV) and an adjacent ash-derived topsoil (26-BRV T, Monte Miranda topsoil) (UTM: X = 746,947 m, Y = 1,640,105 m) already referred by Mourão et al. (2010) (Figs. 2 and 3).

The topsoils samples were collected as follows: circa 2 kg was collected and sifted on-site by hand through a 20 cm diameter nylon sieve with a mesh size of 2 mm into polyethylene bags for transport. It should be noted that these topsoils consist of fine particles smaller than 2 mm in diameter. In the laboratory the samples were dried at 30 °C; samples were mixed and sieved again through a 2 mm nylon sieve (whole sample). After a repeated mixing procedure, samples were quartered by hand. Two portions (circa 100 g each) were separated for analysis: (i) sample T - to be ground and analyzed to obtain the total chemical and mineralogical composition, and (ii) sample A - for grain size fractions separation, weight and analysis (Marques et al., 2011). Two grain size fractions of sample A were obtained by wet sieving: the $\phi > 50$ μm fraction (coarse), and the $\phi < 50$ μm fraction (fine) using deionized water (nylon mesh). This fine fraction was then used to obtain the $\phi < 2$ μm fraction (clay-size) by sedimentation according to Stokes' law (Moore and Reynolds, 1997), after dispersion with sodium hexametaphosphate (1%).

Trace, minor and major elements concentrations of extrusive carbonatites (ash tuff deposit and spatter rampart deposit), as well as of the whole samples and the selected fractions of the topsoils were determined by instrumental neutron activation analysis (INAA). Two reference materials were used in the evaluation of elemental concentrations by INAA: soil GSS-4 and sediment GSD-9 from the Institute of Geophysical and Geochemical Prospecting (IGGE). Reference values were taken from data tabulated by Govindaraju (1994). The samples and standards were prepared for analysis by weighing 200–300 mg of powder into cleaned high-density polyethylene vials. Two aliquots of each standard were used for internal calibration, and standard checks were performed (QA/QC). Short and long irradiations were performed in the core grid of the Portuguese Research Reactor (CTN/IST, at Bobadela) (Fernandes et al., 2010) at a thermal flux of 3.96×10^{12} n cm^{-2} s^{-1}; $\phi_{th}/\phi_{epi} = 96.8$; $\phi_{th}/\phi_{fast} = 29.8$. Two γ-ray spectrometers were used: (1) one consisting of a 150 cm^3 coaxial Ge

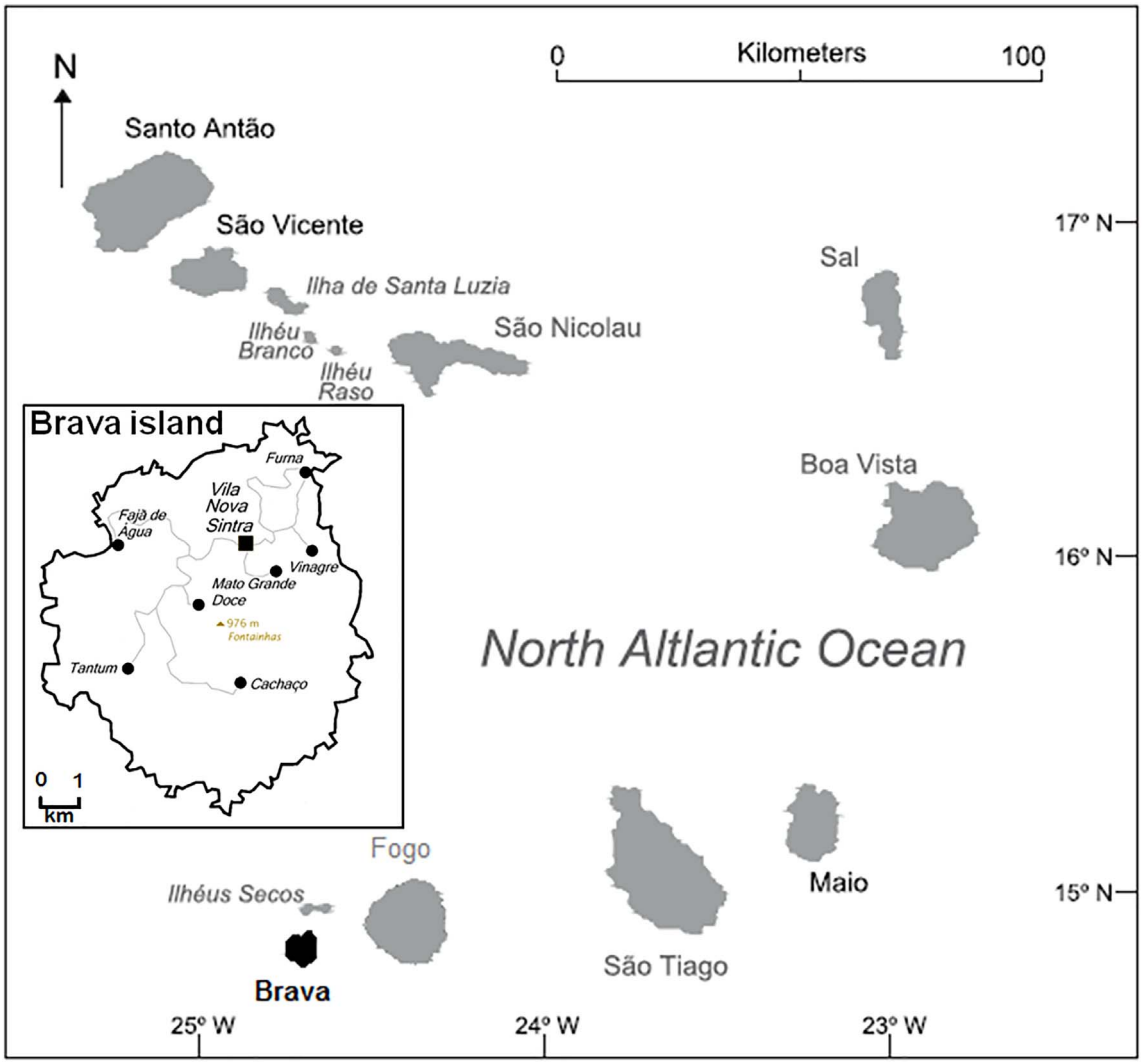

Fig. 1. Location of Brava Island in Cape Verde archipelago and sampling sites (location of Tantum and Monte Miranda, Cachaço) in the detail of Brava Island (see Marques et al., 2016, Fig.1).

detector connected through a Canberra 2020 amplifier to an Accuspec B (Canberra) multichannel analyser. This system had a full width at half maximum (FWHM) of 1.9 keV at 1.33 MeV; and (2) the other consisting of a low energy photon detector (LEPD) connected through a Canberra 2020 amplifier to an Accuspec B (Canberra) multichannel analyser. This system had a FWHM of 300 eV at 5.9 keV and of 550 eV at 122 keV. Corrections for the spectral interference from U fission products in the determination of Ba, REE and Zr were made according to Gouveia et al. (1987) and Martinho et al. (1991). Details of the analytical method may be found in Gouveia et al. (1992), Prudêncio et al. (2006), Kin et al. (1999), and Prudêncio et al. (1986). Different cooling times were selected to determine radionuclides with different half-lives. The chemical contents of Na, K, Fe, Sc, Cr, Mn, Co, Zn, Ga, As, Br, Rb, Zr, Cs, Ba, La, Ce, Nd, Sm, Eu, Tb, Dy, Yb, Lu, Hf, Ta, W, Th and U were obtained. Relative precision and accuracy are, in general, to within 5%, and occasionally within 10%.

The mineralogical composition of the whole samples and the size fractions was determined by X-ray diffraction (XRD) of randomly oriented specimens using a Philips diffractometer, Pro Analytical, with Cu Kα radiation at 40 kV and 35 mA, a step size of 0.5° 2θ/min from 3° to 70° 2θ. Oriented specimens on glass slides of clay-size fraction ($\phi < 2\ \mu m$) were also analyzed by XRD, using the same device from 2° to 30° 2θ with a step size of 1° 2θ/min. The following treatments were performed: air drying, ethylene glycol solvation (EG), and heating (550 °C). The minerals identification was done according to Brindley and Brown (1980), Moore and Reynolds (1997) and Thorez (1976). The diagnostic peaks used were the following: alkali feldspar – 3.24 Å, analcime – 3.43 Å, calcite – 3.03 Å, hematite – 2.68 Å, illite – 10 Å, illite-smectite (I-Sm) – 20-28 Å, kaolinite – 7 Å, magnetite – 2.53 Å, olivine – 2.46 Å, phyllosilicates – 4.45 Å, plagioclase – 3.18 Å, pyroxenes (augite) – 2.99 Å, quartz – 3.35 Å, and smectite (glic.) – 17 Å.

The ^{57}Fe Mössbauer measurements were recorded at 295 and 4 K in transmission mode using a conventional constant acceleration spectrometer and a 25-mCi ^{57}Co source in Rh matrix. The velocity scale was calibrated using an α-Fe foil at room temperature. Isomer shift values, IS, are given relative to this standard. Powdered samples were packed together with lucite powder into perspex holders, in order to obtain homogeneous and isotropic Mössbauer absorbers containing about 5 mg/cm^2 of natural iron. The measurements taken at 4 K were obtained with the samples immersed in liquid He in a bath cryostat. The spectra were fitted to Lorentzian lines using a non-linear least-squares method (Waerenborgh et al., 2000).

4. Results

4.1. Chemical composition

The elemental composition of trace, minor and major elements

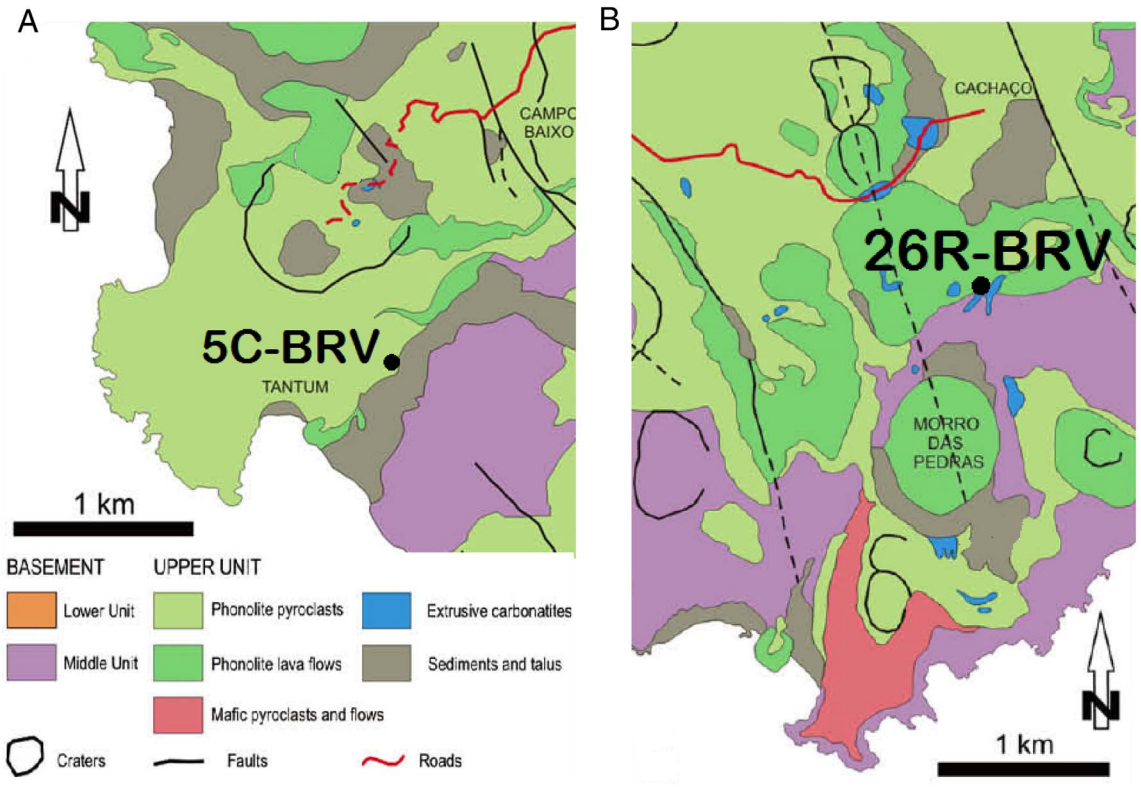

Fig. 2. Location and geological setting of extrusive carbonatite sampling sites in Brava Island, Cape Verde (modified from Madeira et al., 2010), near Tantum (new occurrence; this paper) and Monte Miranda (Cachaço; Mourão et al., 2010).

obtained by INAA in the extrusive carbonatite outcrops (ash/tuff and spatter rampart), as well as in the topsoils - whole samples (T) and in the three selected particle size fractions (of samples A) from Tantum and Monte Miranda are given in Table 1.

The concentration values of each element in the whole sample A were calculated based on the observed chemical concentrations on the coarse and fine fractions and the amounts of these fractions (see Table 1). The variation of the differences between the calculated values (sample A) and the experimental values determined for sample T are different for Tantum and Monte Miranda sites. These variations in increasing order are as follows: (i) Tantum: < 5% for K, Mn, Fe, Sc, Rb, La, Nd, Sm, Eu, Tb, Yb, Hf and Th; 5%–15% for Na, Cr, Co, Br, Zr, Cs, Ba, Ce, Lu, Ta and W; 15%–30% for Ga, As and Dy; and > 30% for Zn, Sb and U; and in (ii) Monte Miranda: < 5% for Na, Mn, Fe, Co, As, Ba, Yb and Lu; 5%–15% for Sc, Cr, Zn, Rb, Zr, Cs, Ce, Eu, Hf, Ta and Th; 15%–30% for K, Ga, La and Dy; > 30% for Br, Sb, Nd, Sm, Tb, W and U.

4.1.1. Rare earth elements patterns

The rare earth elements (REE) patterns were obtained by normalization relative to chondrites (values of Anders and Grevesse (1989) multiplied by 1.36 according Korotev (1996a, 1996b)). Patterns of the ash tuff deposit (5C–BRV) near Tantum and the spatter rampart (26R–BRV) near Monte Miranda are shown in Fig. 4. The REE patterns of topsoils – whole samples (T) and size fractions of sample A are also represented.

In Tantum higher contents and a positive Eu anomaly occur in the ash tuff deposit (5C–BRV) when compared to all topsoil samples. The REE contents and patterns of the topsoil whole sample (5-BRV T) and the size fractions are similar, and no significant Ce or Eu anomalies were observed (Fig. 4a). In opposition, at Monte Miranda (Fig. 4b) the topsoil (whole sample and grain size fractions) has the highest REE content values; REE concentrations increase with the decrease of particle size, and positive Ce and Eu anomalies occur in the clay-size fraction at Monte Miranda.

4.1.2. Chemical distribution in size fractions

When comparing the chemical composition of the different size fractions of the topsoils: (i) in general lower variations are observed in Tantum (Fig. 5a); and (ii) significant enrichments of the majority of the trace elements studied are found in the finer fractions of the Monte Miranda topsoil (Fig. 5b), particularly in the clay-size fraction relative to the fine fraction for Co, Zn, Ga, As, Br, Sb, Ce and W. It is important to emphasize that Sb is the most enriched element studied in the finer fractions of the ash-derived topsoil from Monte Miranda.

4.2. Mineralogy

The mineralogical composition obtained by XRD of the ash tuff near Tantum, the spatter near Monte Miranda, the topsoils whole samples and the different size fractions are given in Table 2. The ash tuff from Tantum (5C–BRV) is mainly composed of calcite, typical of calciocarbonatite formations. A distinct mineralogical association is found for the ash-derived topsoil. The whole sample (5-BRV T) and coarse and fine fractions have similar mineralogical association but with different proportions (see Table 2), being analcime, phyllosilicates, feldspars and calcite the main minerals; iron oxides, quartz and olivine are also detected. The clay-size fraction consists of clay minerals, mainly smectite and illite; trace amounts of kaolinite and mixed-layer I-Sm are also identified. Analcime and calcite were also found in the oriented sample run on the diffractometer (air dried) between 2° to 30° 2θ.

The Monte Miranda spatter (26R-BRV) and the adjoining ash derived topsoil whole sample (26-BRV T) are mainly composed of calcite. Magnetite, subordinate quartz, and trace amounts of phyllosilicates (mainly micas) are also detected. Calcite is found in all the studied size fractions and its proportion decreases with the particle size. Illite is the main clay mineral, associated to traces amounts of smectite and mixed-layer I-Sm.

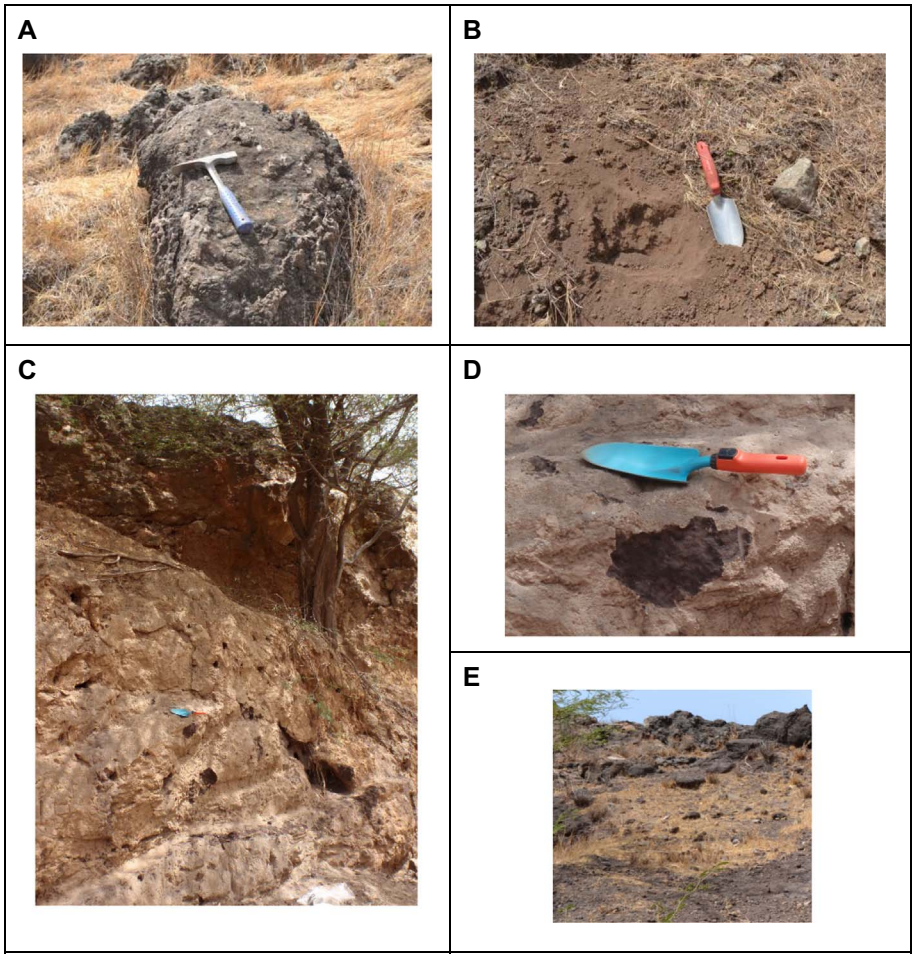

Fig. 3. Field photographs of extrusive carbonatite outcrops from Brava Island (Cape Verde): Monte Miranda - (a) proximal spatter rampart, (b) carbonatite ash-derived topsoil; Tantum - (c) a profile with a small terrace (where a tree has grown) exposing phonolitic pyroclasts on the top of a carbonatite ash fall deposit, (d) a detail of the ash fall deposit (dark color where surface alteration was removed), (e) carbonatite outcrop near Tantum.

4.3. Mössbauer spectroscopy

In the Mössbauer spectra of samples of the outcrop of the ash fall deposit near Tantum (5C–BRV) as well as of samples of the Monte Miranda spatter (26R-BRV) and the corresponding ash-derived topsoil (26-BRV T) the typical pattern of magnetite predominates (Figs. 6 and 7). The estimated isomer shift (IS) and magnetic hyperfine fields (B_{hf}) summarized in Table 3 confirm this assignment (Abreu et al., 1988; Vandenberghe et al., 2000).

In the spectra of the Tantum topsoil (5-BRV T and 5-BRV A < 50 μm) no magnetite is observed (see Fig. 6). In the fine fraction, at room temperature, two doublets, one consistent with Fe^{2+} in silicates and the other with Fe^{3+} in both silicates and nano-size-oxides, are detected (Table 3). The presence of these nano-size- oxides is confirmed by the spectrum taken at 4 K (Fig. 6) where a six-peak pattern with broad peaks is clearly observed. This pattern may be fitted with two sextets. The fitted parameters suggest that the sextet with higher B_{hf} may be attributed to maghemite and the remaining one to poorly crystallized hematite with Fe partially substituted by impurity atoms, namely Al (Marques et al., 2014a, 2014b; Murad, 1998; Vandenberghe et al., 1990, 2000). The impurities and small particle effects on the spectrum of the hematite in the soil sample explain the suppression of the Morin transition and the lower B_{hf} when compared to pure bulk hematite. In the clay-size fraction of Tantum topsoil the same nano-size- Fe^{3+} oxides are detected. The only difference relative to the whole and fine fraction samples is the absence of Fe^{2+} containing phyllosilicates.

The spectrum of the ϕ < 50 μm fraction of the Monte Miranda topsoil reveals that this sample mainly consists of magnetite as found in the whole sample (26-BRV T). A doublet with parameters typical of Fe^{3+} in phyllosilicates and nano-size-Fe^{3+} oxides (Murad, 1998) is also present in the above referred spectra. Magnetite is only absent in the clay-size fraction. In this fraction Fe is only present in the 3 + oxidation state in the structure of phyllosilicates and in nano-size-oxides (Fig. 7).

5. Discussion

The chemical and mineralogical results obtained in this work confirm that high contents of W along with high contents of REE, Ba, Th and U in topsoils from Brava Island may be used as an indicator of underlying and/or nearby occurrence of carbonatitic materials, in particular of extrusive carbonatites, sometimes difficult to identify in the field (see also Marques et al., 2016). In the case of the Tantum topsoil, despite the contribution of phonolitic pyroclasts from the slope above, these features prevail along with significant amounts of calcite, which lead to the identification of a new 3 m thick carbonatite ash tuff outcrop (see Fig. 3c, d, e). This ash tuff (5C-BRV) is an extrusive calciocarbonatite belonging to the younger volcanic sequence of Brava, chemically similar to those reported by Mourão et al. (2010) (particularly sample CY-221), with high REE contents and similar patterns, but a more significant positive Eu anomaly (Eu/Eu* = 1.21). In the Monte Miranda spatter a significant positive anomaly also occurs (Eu/Eu* = 1.33), which can be explained by the easy Eu reduction to a divalent species, and incorporation on the Ca lattice site (Möller, 1998;

Table 1
Chemical contents of the ash tuff deposit near Tantum (5C–BRV), the Monte Miranda spatter (26R-BRV), the whole samples (T) and the different size fractions of topsoils from Brava Island (Cape Verde), obtained by INAA (major elements are expressed in % oxide and trace elements in mg/kg). (The chemical contents calculated for the whole sample A and the amount of fine and coarse fractions (%) are also given).

Location	Tantum						Monte Miranda					
Description	Ash tuff	Topsoil					Spatter rampart	Topsoil				
		Whole sample		Fraction				Whole sample		Fraction		
Reference	5C-BRV	5-BRV T[a]	5-BRV A[b]	5-BRVA > 50 μm (43%)	5-BRVA < 50 μm (57%)	5-BRVA < 2 μm	26R–BRV	26-BRV T[a]	26-BRV A[b]	26-BRV A > 50 μm (71%)	26-BRV A < 50 μm (29%)	26-BRV A < 2 μm
Na_2O	0.478	2.52	2.69	3.10	2.38	3.48	0.211	0.440	0.458	0.512	0.327	0.277
K_2O	0.932	1.73	1.66	1.92	1.46	1.54	0.105	0.507	0.644	0.598	0.757	0.788
MnO	1.14	0.281	0.273	0.281	0.267	0.288	0.817	1.04	0.991	0.836	1.37	1.563
Fe_2O_3T	10.8	10.4	10.6	11.6	9.78	8.97	5.57	9.23	8.80	6.71	13.9	7.18
Sc	2.00	16.6	16.6	20.1	13.9	11.8	0.58	1.45	1.59	1.55	1.68	2.39
Cr	13.1	73.1	65.1	79.5	54.3	47.3	13.2	21.0	23.2	23.1	23.4	38.6
Co	4.97	31.6	34.6	28.0	39.6	44.8	3.07	5.61	5.88	4.72	8.74	14.4
Zn	70.2	125	174	173	174	168	205	312	352	407	217	1240
Ga	39.2	26.1	21.0	14.4	26.0	29.4	9.32	27.6	20.7	15.7	32.8	97.8
As	3.08	4.46	5.77	5.94	5.65	5.11	1.97	1.96	2.06	1.60	3.20	12.6
Br	2.32	2.36	2.69	3.72	1.92	4.84	3.91	5.12	3.19	2.94	3.81	16.7
Rb	18.1	78.4	79.2	74.0	83.2	78.8	29.4	69.4	76.5	55.9	127	202
Zr	682	495	422	427	419	380	388	669	607	519	822	1039
Sb	0.263	0.267	0.369	0.379	0.361	0.318	0.156	0.216	0.832	0.155	2.49	39.9
Cs	0.958	1.59	1.73	1.58	1.84	2.11	0.752	1.40	1.59	1.27	2.37	3.13
Ba	5537	834	759	876	671	462	13,188	8274	8661	7820	10,719	8994
La	1070	149	147	126	163	161	517	813	952	798	1330	2250
Ce	1827	265	290	286	293	292	978	1450	1649	1179	2798	6658
Nd	707	122	127	111	139	125	348	448	612	530	812	1298
Sm	80.2	20.3	19.4	17.7	20.6	19.5	35.3	53.2	76.9	70.0	93.8	104
Eu	32.1	6.13	6.10	5.67	6.43	5.95	14.6	23.1	25.1	22.3	32.1	41.6
Tb	11.9	2.29	2.19	2.10	2.25	2.15	4.00	6.29	8.41	7.07	11.7	11.3
Dy	64.0	11.3	9.04	8.70	9.30	11.3	23.1	31.9	37.5	32.6	49.5	55.0
Yb	26.7	4.60	4.57	4.46	4.65	3.88	11.3	16.1	16.9	15.5	20.4	24.2
Lu	3.33	0.527	0.493	0.484	0.499	0.439	1.19	1.78	1.79	1.64	2.14	2.78
Hf	1.40	8.11	8.12	8.89	7.54	7.06	0.917	2.21	1.87	1.66	2.38	2.69
Ta	1.63	6.31	6.91	5.98	7.62	3.66	1.31	1.89	1.76	1.61	2.12	0.76
W	5.60	7.12	6.54	5.33	7.46	6.23	5.69	7.98	10.6	8.48	15.7	100
Th	55.7	12.1	12.4	11.4	13.2	13.9	21.5	34.7	40.2	27.6	71.2	94.8
U	10.5	2.16	4.19	3.72	4.55	2.86	2.18	3.04	4.52	3.52	6.96	8.23

[a] Experimental data from Marques et al. (2016).
[b] Calculated values.

Marques et al., 2017). A similar positive anomaly was found in Grønnedal-Ika calcite carbonatites by Halama et al. (2005). Despite some chemical variations found between the newly reported Tantum extrusive carbonatite outcrop and the spatter of Monte Miranda, similar REE patterns and high W concentrations (up to 5.7 mg/kg) occur. Concerning the other trace elements concentrations, Tantum carbonatite has significant higher contents of Sc, Ga, REE, Th and U, while in Monte Miranda Br, Rb and particularly Zn and Ba are present in high concentrations. Calcite dominates and iron species are identical in both extrusive carbonatite outcrops. Magnetite is the major iron form in Tantum ash tuff and in Monte Miranda spatter (corresponding to 93% and 85% of the total iron respectively).

The chemical differences found between the whole samples of the topsoils of both sites, may be mainly explained by differences in the parent material and in the degree of alteration/oxidation: (i) Tantum – mixture of phonolite pyroclasts and carbonatite ash tuff and (ii) Monte Miranda – mostly carbonatite ash. Accordingly, lower proportions of calcite were found in Tantum where phyllosilicates dominate and analcime, alkali feldspars, olivine and iron oxides were also detected by XRD. On the other hand, calcite dominates in the Monte Miranda topsoil. Mössbauer data clearly show that magnetite occurs in the Monte Miranda topsoil but is absent in Tantum topsoil where it has been completely oxidized to maghemite and poorly crystalline hematite.

Concerning the chemical elements distribution in the different size fractions of the topsoils, no significant variations are observed in Tantum. In Monte Miranda's topsoil formed by weathering of carbonatite ash, the opposite occurs for the majority of the elements studied, particularly for Sb and W in the clay-size fraction (see Fig. 5b). Although XRD and Mössbauer did not identify Sb and W mineral carriers, these elements may occur due to hydrothermal activity (Ashley et al., 2003; Koutsospyros et al., 2006) or precipitate as stibnite and wolframite respectively, in the vicinity of volcanic conduits, along with magnetite (Stoppa et al., 2016; Zhu et al., 2011). Considering the low Sb concentrations in the earth's crust, the presence of this element in such high concentration in the clay-size fraction (39.9 mg/kg) is certainly related to the volcanic processes. In fact, according to Miravet et al. (2007) the volcanic activity is responsible for 3–5% of global antimony emissions to the air, and Sb may be present in high concentrations in volcanic ashes and air-transported even from distant regions. Weathering and pedogenic processes can lead to enrichment in Sb, according to Reimann et al. (2010). The enrichment in Sb in topsoils may be explained by its strong tendency to be sorbed by hydrous oxides (of Fe and Mn), clay minerals and organic matter. The presence of significant Sb amounts in the fine-sized particles may contribute to its accumulation in plants both by absorption and by dust deposition onto the plant leaves. A significant enrichment of W was also found at Monte Miranda, particularly in the clay-size fraction of the topsoil (100 mg/

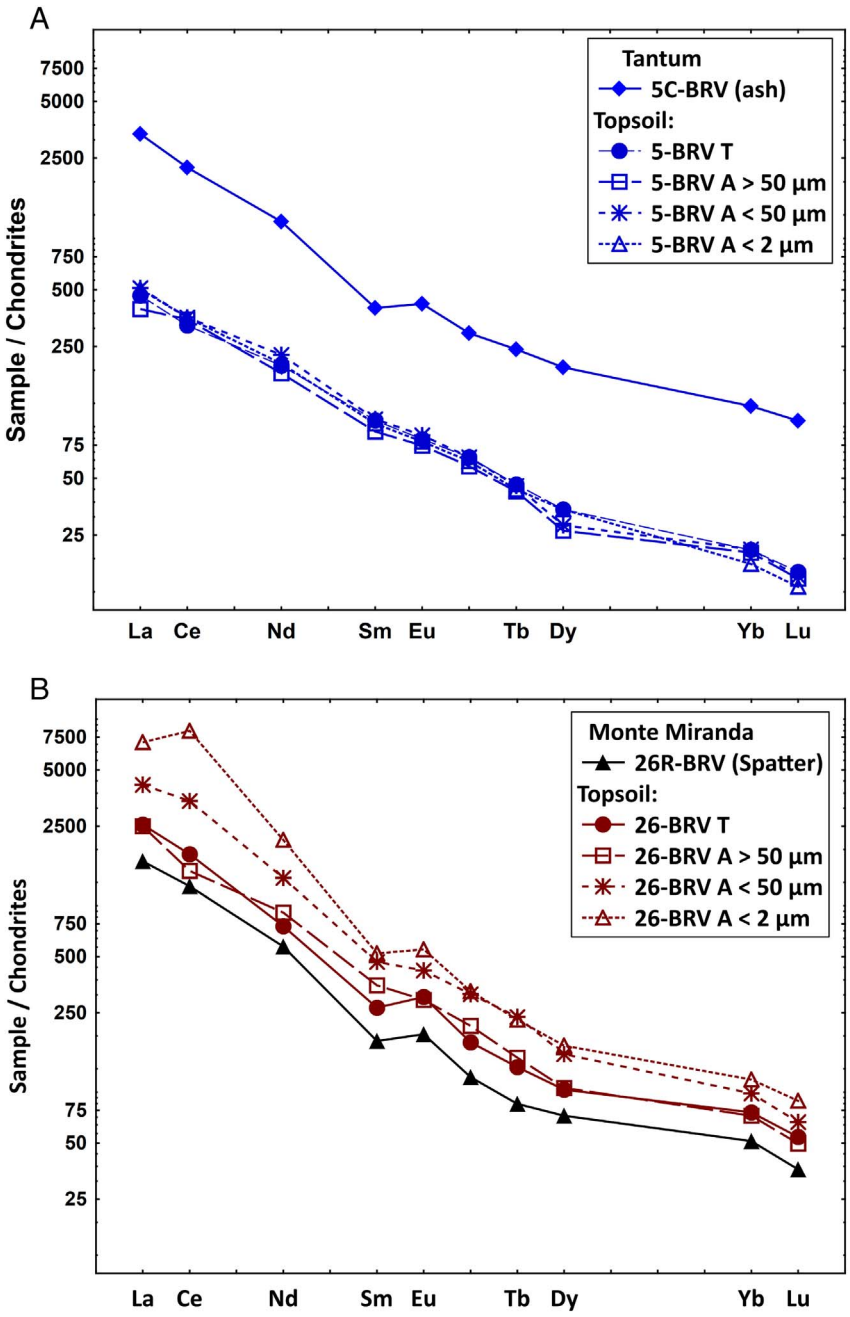

Fig. 4. REE patterns of the carbonatite, whole samples (T) and size fractions from the Tantum (a) and the Monte Miranda (b) outcrops, Brava Island (Cape Verde).

kg). An enrichment of W may occur in natural aquatic systems, in the surface or underground, in areas of hydrothermal activity as reported by Koutsospyros et al. (2006). This author also reports that W appears to be absorbed by plants from soils, water or atmospheric systems and even be translocated to several parts of the plant anatomy. This could be an environmental issue in the case of Brava Island taking into account that W may prevail in the ecosystems in different interchangeable forms making diverse soluble complexes, including with halogens like fluorine, an element abundant in carbonatite rocks (e.g. Mourão et al., 2012b). Traub et al. (2009) showed that a concentration of 1.4 mg/kg of F in drinking water occurs in Brava Island. As this element may be deposited in the skeleton and teeth, some degree of enamel mottling of the inhabitants dentition was found by these authors. The high W concentrations found in the fine particles soils, its mobility and known ability to form complexes with F may lead to a higher concentration of this element in drinking water, constituting a natural hazard that needs further investigation.

The chemical heterogeneity found within each topsoil sample studied in the present work may be mainly explained by the low degree of weathering of very recent extrusive carbonatite parent rocks (< 0.25 Ma) in Brava Island under a semi-arid climate. Prudêncio et al. (1995) used a similar laboratorial protocol to obtain the whole sample and different size fractions, as well as the same analytical technique for the chemical information of soils developed on basaltic rocks from the Lisbon Volcanic Complex (Portugal) (≈ 72 Ma) which have been exposed for a much longer period of time.

The positive Eu anomaly observed in all the studied size fractions of the Monte Miranda topsoil is most probably mainly inherited from the parent rock. Also, a concentration of REE in the particles of small dimensions occurs, which may be partially explained by the presence of REE-bearing primary minerals and/or by their incorporation/adsorption on clay minerals or on iron oxides (Prudêncio et al., 2010). In fact,

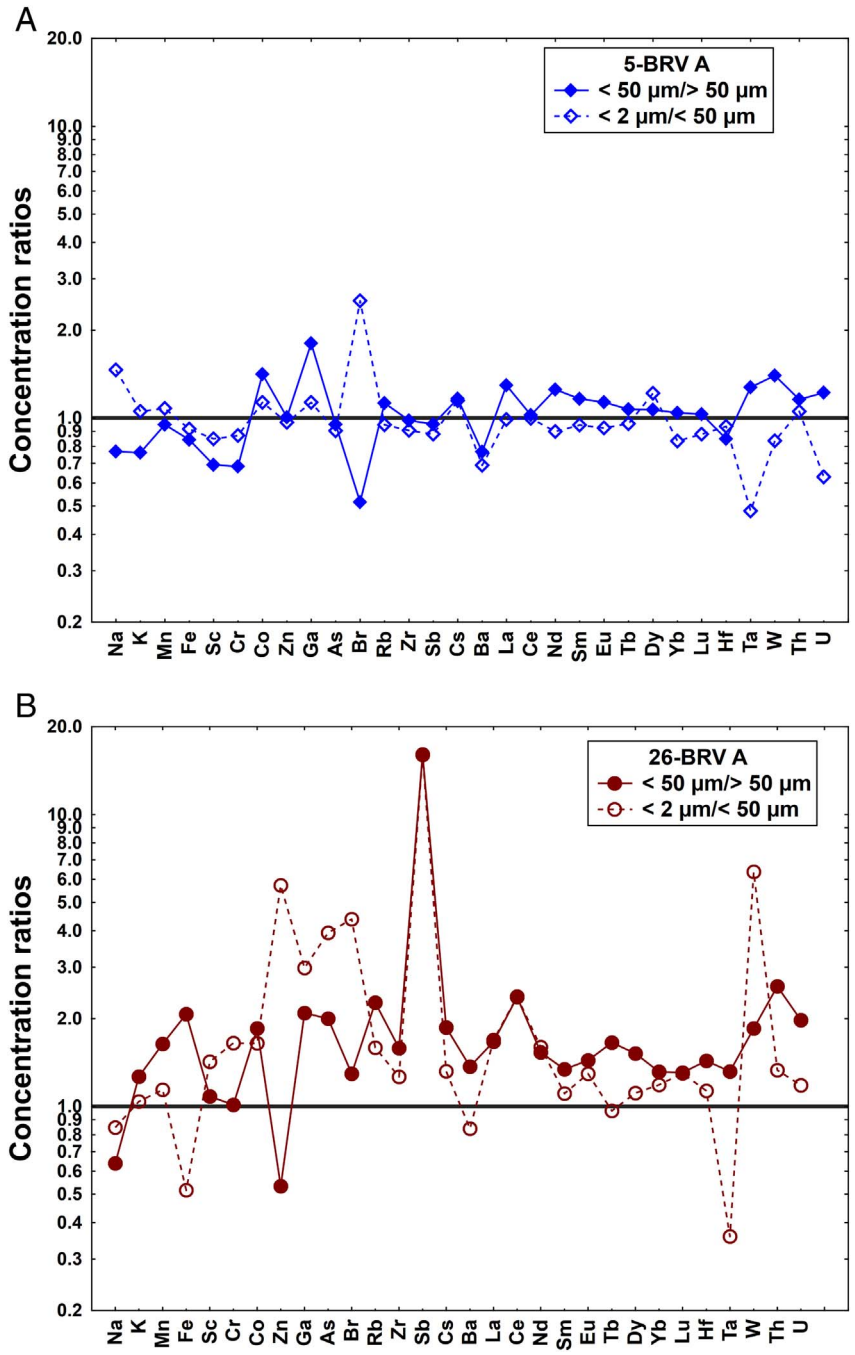

Fig. 5. Concentration ratios of the fine fraction relative to coarse fraction and the clay-size fraction relative to the fine fraction of topsoils from Tantum (a) and Monte Miranda (b), Brava Island (Cape Verde).

Table 2
Mineralogical associations obtained by XRD of the studied ash tuff deposit, spatter, the whole samples (T) and different size fractions of the Brava topsoils (Cape Verde).

	Reference	Mineralogical association
Tantum	5C–BRV	Calcite ≫ magnetite > quartz > pyroxenes
	5-BRV T	Phyllosilicates ≈ calcite > analcime ≫ K-Feldspars ≈ olivine > quartz ≈ plagioclase > hematite
	5-BRV A > 50 µm	Plagioclase > > calcite > phyllosilicates > quartz > > K-Feldspars > pyroxenes > analcime > olivine ≈ hematite
	5-BRV A < 50 µm	Phyllosilicates ≈ analcime ≈ calcite ≈ K-Feldspars ≈ plagioclase > quartz ≈ hematite ≈ olivine
	5-BRV A < 2 µm	Smectite > illite > kaolinite (traces) ≈ I-Sm (traces) (+ analcime > Calcite)
Monte Miranda	26R–BRV	Calcite ≫ magnetite > quartz > phyllosilicates (traces)
	26-BRV T	Calcite ≫ magnetite > pyroxenes ≈ phyllosilicates > quartz ≈ K-Feldspars (traces)
	26-BRV A > 50 µm	Calcite ≫ magnetite > K-Feldspars ≈ pyroxenes > quartz > phyllosilicates (traces)
	26-BRV A < 50 µm	Calcite ≫ phyllosilicates > magnetite > pyroxenes > K-Feldspars > quartz (traces)
	26-BRV A < 2 µm	Illite ≫ smectite (traces) (+ Calcite)

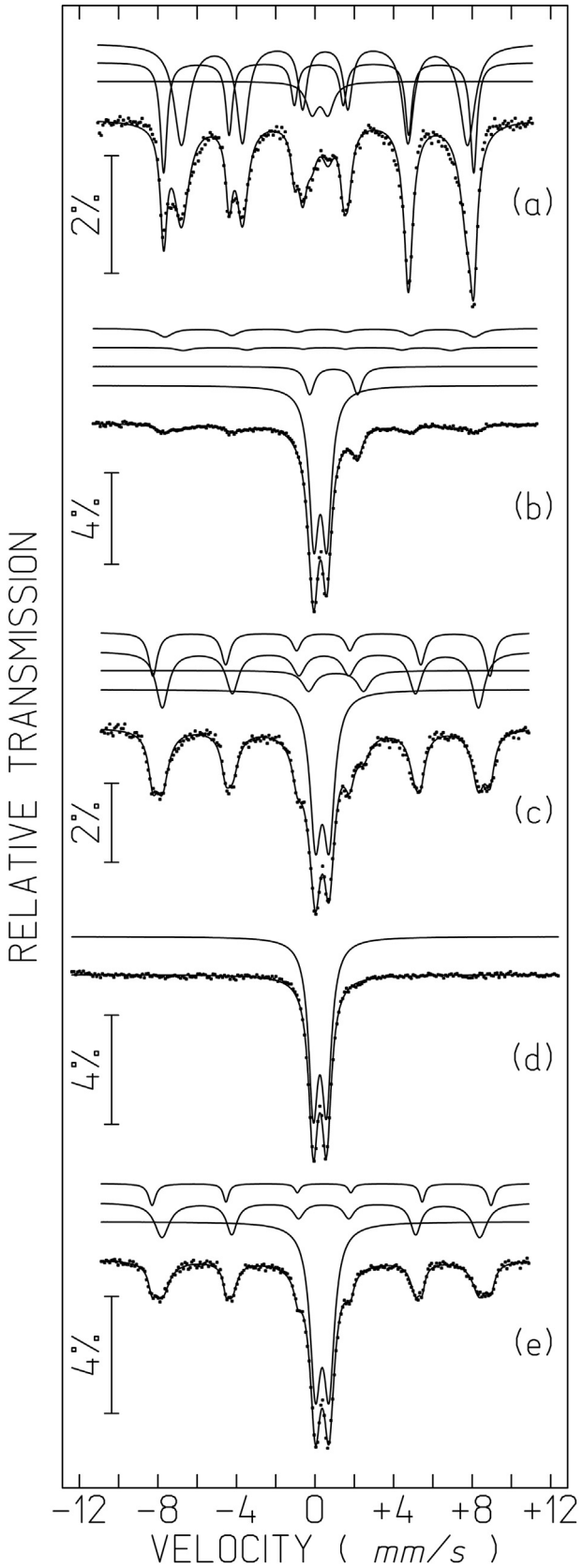

Fig. 6. Mössbauer spectra of (a) 5C–BRV at 295K, (b) 5-BRV T at 295 K, (c) 5-BRV T at 4 K, (d) 5-BRV A < 2 μm fraction at 295 K and (e) 5-BRV A < 2 μm fraction at 4 K, of carbonatitic soils from Brava Island (Cape Verde). The lines over the experimental points are the sum of fitted doublets and or sextets (shown slightly shifted for clarity) attributed to the Fe species referred in the text and in Table 3.

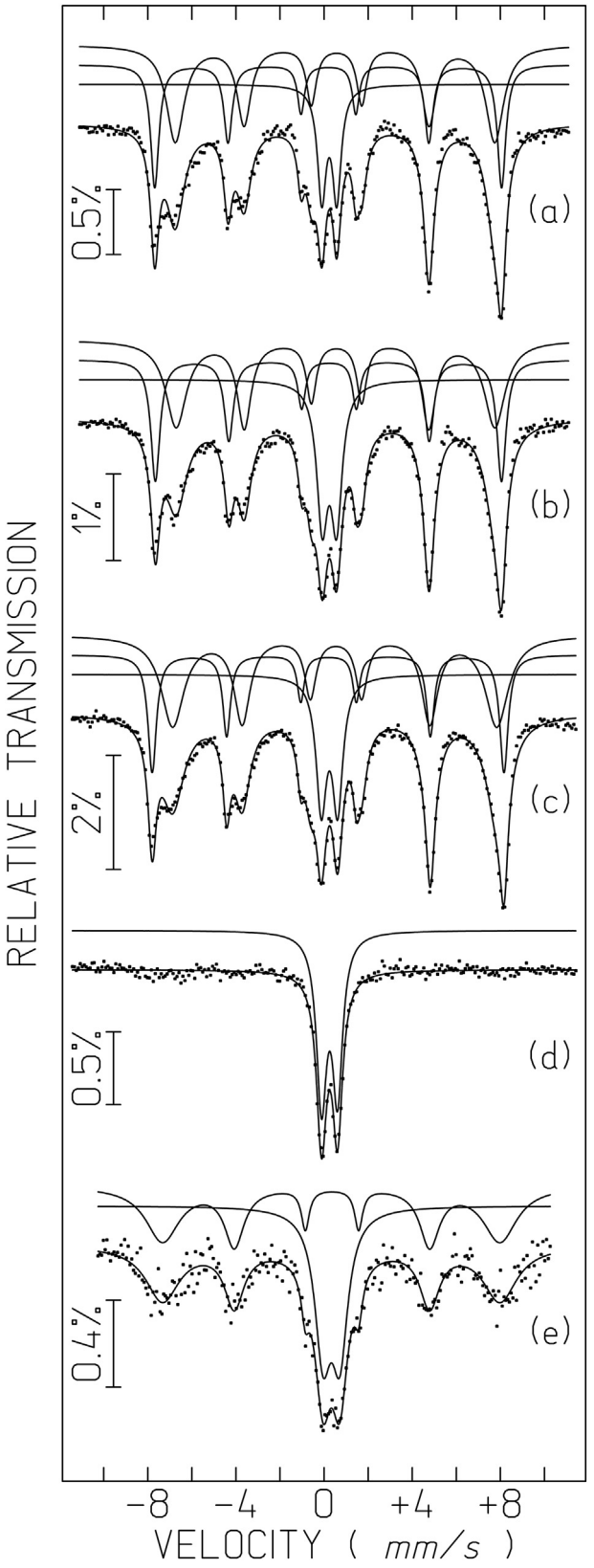

Fig. 7. Mössbauer spectra of (a) 26R–BRV, (b) 26-BRV T, (c) 26-BRV A < 50 μm fraction, (d) 26-BRV A < 2 μm fraction at 295 K, and (e) spectrum of 26-BRV A < 2 μm fraction at 4 K, of carbonatitic soils from Brava Island (Cape Verde). The lines over the experimental points are the sum of fitted doublets and or sextets (shown slightly shifted for clarity) attributed to the Fe species referred in the text and in Table 3.

Table 3
Estimated parameters from the Mössbauer spectra, taken at 295 K and 4 K, of the outcrop of the ash tuff deposit near Tantum (5C-BRV), the Monte Miranda spatter (26R-BRV), the whole samples (T) and the different size fractions of the adjoining topsoils of Brava Island (Cape Verde).

Reference sample	T	Fe species	IS	QS, ε	B_{hf}	I
5C–BRV	295 K	Fe^{3+} silicates, nso	0.36	0.82	–	7%
		Fe^{3+} $Fe_{3-x}O_4$	0.30	−0.01	48.9	30%
		$Fe^{2.5+}$ $Fe_{3-x}O_4$	0.61	−0.04	45.2	63%
5-BRV T (whole sample)	295 K	Fe^{3+} silicates, nso	0.38	0.66	–	67%
		Fe^{2+} silicates	1.06	2.43	–	10%
		Fe^{3+} nso	0.40	−0.37	42.3	4%
		Fe^{3+} nso	0.39	−0.09	48.9	13%
	4 K	Fe^{3+} silicates	0.48	0.70	–	37%
		Fe^{2+} silicates	1.18	2.80	–	7%
		Fe^{3+} α-Fe_2O_3	0.48	−0.11	50.0	38%
		Fe^{3+} γ Fe_2O_3	0.49	−0.10	53.3	18%
5-BRV A < 50 μm	295 K	Fe^{3+} silicates, nso	0.37	0.67	–	79%
		Fe^{2+} silicates	1.06	2.54	–	6%
		Fe^{3+} nso	0.39	−0.31	40.8	3%
		Fe^{3+} nso	0.37	−0.07	48.1	12%
5-BRV A < 2 μm	295 K	Fe^{3+} phyllosilicates, nso	0.36	0.67	–	100%
	4 K	Fe^{3+} phyllosilicates	0.48	0.70	–	56%
		Fe^{3+} α-Fe_2O_3	0.48	−0.15	50.1	34%
		Fe^{3+} γ Fe_2O_3	0.50	−0.13	53.5	10%
26R-BRV	295 K	Fe^{3+} silicates, nso	0.35	0.68	–	15%
		Fe^{3+} $Fe_{3-x}O_4$	0.31	−0.01	48.8	32%
		$Fe^{2.5+}$ $Fe_{3-x}O_4$	0.64	−0.07	45.0	53%
26-BRV T (whole sample)	295 K	Fe^{3+} silicates, nso	0.35	0.65	–	21%
		Fe^{3+} $Fe_{3-x}O_4$	0.32	−0.03	48.7	30%
		$Fe^{2.5+}$ $Fe_{3-x}O_4$	0.65	−0.04	44.9	49%
26-BRV A < 50 μm	295 K	Fe^{3+} silicates, nso	0.36	0.74	–	18%
		Fe^{3+} $Fe_{3-x}O_4$	0.30	−0.02	49.5	26%
		$Fe^{2.5+}$ $Fe_{3-x}O_4$	0.62	−0.06	45.6	56%
26-BRV A < 2 μm	295 K	Fe^{3+} phyllosilicates, nso	0.36	0.72	–	100%
	4 K	Fe^{3+} phyllosilicates	0.46	0.77		40%
		Fe^{3+} nso	0.48	−0.03	−47.5	60%

nso nano-size-Fe^{3+} oxides. IS (mm/s) isomer shift relative to metallic α-Fe at 295 K; QS (mm/s) quadrupole splitting. $\varepsilon = (e^2V_{zz}Q/4)$ $(3\cos^2\theta - 1)$ (mm/s) quadrupole shift estimated for the sextets. B_{hf} (tesla) magnetic hyperfine field. Estimated errors ≤ 0.02 mm/s for IS, QS, ε, < 0.2 T for B_{hf} and < 2% for I.

the significant enrichment of LREE, particularly Ce in the clay-size fraction of this topsoil, may be due to the presence of REE-containing minerals rich in LREE, particularly Ce (cerite) or to weathering processes with oxidizing conditions and formation of cerianite, which is in agreement with the Mössbauer results obtained for this sample. In fact, all the iron present in the clay-size fraction is in the oxidation state 3^+, and is included in clay minerals or nano-size-oxide particles. The higher positive Eu anomaly in the clay-size fraction is probably inherited from a higher proportion of Eu^{2+} relative to the trivalent REE release after the breakdown of calcite and further incorporation in clay minerals (Marques et al., 2014a; Prudêncio et al., 2011). In the whole sample and in the ϕ < 50 μm fraction, approximately 80% of the Fe remains as magnetite. This oxide is only absent in the clay-size fraction where Fe is found to be completely oxidized both in phyllosilicates and in nano-size-Fe^{3+} oxides. This suggests that only mild weathering of magnetite has occurred in Monte Miranda.

It should be noted that magnetite is the major iron form in the extrusive carbonatite ash and spatter deposits of Tantum and Monte Miranda. According to Hoernle et al. (2002) and Mourão et al. (2010), the extrusive carbonatites of Brava Island are very recent, which associated with the semi-arid climate leads to a low degree of weathering explaining the good preservation of magnetite in Monte Miranda topsoil.

6. Conclusions

The newly reported extrusive carbonatite ash tuff deposit located near Tantum in Brava Island corresponds to a calciocarbonatite with high W and REE concentrations, and a positive Eu anomaly similar to the Monte Miranda spatter deposit. Iron species are identical in both extrusive carbonatite outcrops, magnetite being the major iron form. High W and REE concentrations and the presence of calcite in topsoils may serve as tracers for extrusive carbonatite occurrences. High concentrations of Mn, Ba and Th are also found in the topsoil developed by weathering of carbonatite ash.

The elemental distribution in the different size fractions of the topsoil developed on carbonatite ash mixed with phonolite pyroclastic material (Tantum) vary much less than in the Monte Miranda topsoil whose parent material consists mostly of extrusive carbonatite ash. In this topsoil Sb and W are the most enriched elements in the finer particles. The significant compositional heterogeneity of the shallow volcanic incipient topsoils developed on extrusive carbonatites of both sites (Tantum and Monte Miranda) may justify further detailed studies of topsoils with contribution of these carbonatites, since a large number of outcrops occur in Brava Island. Also, despite the low number of topsoils studied, the high contents of certain chemical elements should be subject of further investigations on their mobility, bioavailability and other issues of environmental health.

Acknowledgments

Grateful acknowledgments are made to financial support from project UID/GEO/04035/2013 funded by FCT (Portugal). C2TN/IST authors gratefully acknowledge the FCT (Portuguese Science and Technology Foundation) support through the UID/Multi/04349/2013 project. Acknowledgments are made to the Laboratory of Nuclear Engineering (LEN) and also to the staff of the Portuguese Research Reactor (RPI) of CTN/IST for their assistance with the neutron irradiations. The authors would like to thank Câmara Municipal da Brava, Vila Nova Sintra (Brava Island, Cape Verde), for the support in fieldwork and sampling.

References

Abreu, M.M., Figueiredo, M.O., Waerenborgh, J.C., Cabral, J.M.P., 1988. Oriented overgrowth of acicular maghemite crystals on quartz. Clay Miner. 23, 357–365.
Allègre, C.J., Pineau, F., Bernat, M., Javoy, M., 1971. Evidence for the occurrence of carbonatites on Cape Verde and Canary Islands. Nature Phys. Sci. 233, 103–104.
Anders, E., Grevesse, N., 1989. Abundances of the elements: meteoritic and solar. Geochim. Cosmochim. Acta 53, 197–214.
Ashley, P.M., Craw, D., Graham, B.P., Chappell, D.A., 2003. Environmental mobility of antimony around mesothermal stibnite deposits, New South Wales, Australia and southern New Zealand. J. Geochem. Explor. 77, 1–14.
Assunção, C.F.T., Machado, F., Gomes, R.A.D., 1965. On the occurrence of carbonatites in the Cape Verde Islands. Bol. Soc. Geol. Port. 16, 179–188.
Bebiano, J.B., 1932. A geologia do arquipélago de Cabo Verde. Comum. Serv. Geol. Port. 18, 1–275.
Bell, K., Simonetti, A., 2010. Source of parental melts to carbonatites–critical isotopic constraints. Mineral. Petrol. 98, 77–89.
Brindley, G.W., Brown, G., 1980. Crystal Structures of Clay Minerals and their X-ray Identification. Mineralogical Society, London.
Darnley, A.G., Bjorklund, A., Bölviken, B., Gustavsson, N., Koval, P.V., Plant, J.A., Steenfelt, A., Tauchid, M., Xuejing, X., 1995. A global geochemical database for environmental and resource management. In: Recommendations for International Geochemical Mapping Final Report of IGCP Project 259. Publishing, UNESCO.
De Ignacio, C., Munõz, M., Sagredo, J., 2012. Carbonatites and associated nephelinites from São Vicente, Cape Verde Islands. Mineral. Mag. 76 (2), 311–355.
Doucelance, R., Hammouda, T., Moreira, M., Martins, J.C., 2010. Geochemical constrains on depth of origin of oceanic carbonatites: the Cape Verde case. Geochim. Cosmochim. Acta 74, 7261–7282.
Ernst, R., Bell, K., 2010. Large igneous provinces (LIPs) and carbonatites. Mineral. Petrol. 98, 55–76.
Fernandes, A.C., Santos, J.P., Marques, J.G., Kling, A., Ramos, A.R., Barradas, N.P., 2010. Validation of the Monte Carlo model supporting core conversion of the Portuguese Research Reactor (RPI) for neutron fluence rate determinations. Ann. Nucl. Energy 37, 1139–1145.
Fúster, J.M., Cendrero, A., Gastesi, P., Ibarrola, E., López-Ruiz, J., 1968. Geología y

Volcanología de las Islas Canarias. Fuerteventura, Instituto Lucas Mallada, CSIC, Madrid (239 p.).
Gouveia, M.A., Prudêncio, M.I., Freitas, M.C., Martinho, E., Cabral, J.M.P., 1987. Interference from uranium fission products in the determination of rare earths, zirconium and ruthenium by instrumental neutron activation analysis in rocks and minerals. J. Radioanal. Nucl. Chem. 2, 309–318 (articles 14).
Gouveia, M.A., Prudêncio, M.I., Morgado, I., Cabral, J.M.P., 1992. New data on the GSJ reference rocks JB-1a and JG-1a by instrumental neutron activation analysis. J. Radioanal. Nucl. Chem. 158 (1), 115–120.
Govindaraju, K., 1994. Compilation of working values and sample description for 383 geostandards. Geostand. Newslett. 18, 1–158.
Halama, R., Vennemann, T., Siebel, W., Markl, G., 2005. The Grønnedal-Ika carbonatite-syenite complex, South Greenland: carbonatite formation by liquid immiscibility. J. Petrol. 46, 191–217.
Hoernle, K., Tilton, G., Le Bas, M.J., Duggen, S., Garbe-Schönberg, D., 2002. Geochemistry of oceanic carbonatites compared with continental carbonatites: mantle recycling of oceanic crustal carbonate. Contrib. Mineral. Petrol. 142, 520–542.
Jones, A.P., Genge, M., Carmody, L., 2013. Carbonate melts and carbonatites. Rev. Mineral. Geochem. 75, 289–322.
Jorgensen, J.O., Holm, P.M., 2002. Temporal variation and carbonatite contamination in primitive ocean island volcanics from São Vicente, Cape Verde Islands. Chem. Geol. 192, 249–267.
Kin, F.D., Prudêncio, M.I., Gouveia, M.A., Magnusson, E., 1999. Determination of rare earth elements in geological samples: a comparative study of instrumental neutron activation analysis and inductively coupled plasma mass spectrometry. Geostand. Newslett. 23 (1), 47–58.
Kogarko, L.N., 1993. Geochemical characteristics of oceanic carbonatites from the Cape Verde Islands. S. Afr. J. Geol. 96, 119–125.
Korotev, R.L., 1996a. A self-consistent compilation of elemental concentration data for 93 geochemical reference samples. Geostand. Newslett. 20, 217–245.
Korotev, R.L., 1996b. On the relationship between the Apollo 16 ancient regolith breccias and feldspathic fragmental breccias, and the composition of the prebasin crust in the central highlands of the moon. Meteorit. Planet. Sci. 31, 403–412.
Koutsospyros, A., Braida, W., Christodoulatos, C., Dermatas, D., Strigul, N., 2006. A review of tungsten: from environmental obscurity to scrutiny. J. Hazard. Mater. 136, 1–19.
Le Maitre, R.W., 2002. Igneous Rocks. A Classification and Glossary of Terms. Recommendations of the International Union of Geological Sciences Subcommission on the Systematics of Igneous Rocks. Cambridge University Press, Cambridge (236 pp.).
Machado, F., Azeredo Leme, J., Monjardino, J., Seita, M.F., 1968. Carta geológica de Cabo Verde, notícia explicativa da Ilha Brava e dos Ilhéus Secos. Garcia de Orta 16, 123–130.
Madeira, J., Mata, J., Mourão, C., Brum da Silveira, A., Martins, S., Ramalho, R., Hoffmann, D.L., 2010. Volcano-stratigraphic and structural evolution of Brava Island (Cape Verde) based on 40Ar/39Ar, U-Th and field constraints. J. Volcanol. Geotherm. Res. 196, 219–235.
Marques, R., Prudêncio, M.I., Dias, M.I., Rocha, F., 2011. Patterns of rare earth and other trace elements in different size fractions of clays of Campanian–Maastrichtian deposits from the Portuguese western margin (Aveiro and Taveiro formations). Chem. Erde 71, 337–347.
Marques, R., Prudêncio, M.I., Waerenborgh, J.C., Rocha, F., Dias, M.I., Ruiz, F., Ferreira da Silva, E., Abad, M., Muñoz, A.M., 2014a. Origin of reddening in a paleosol buried by lava flows in Fogo Island (Cape Verde). J. Afr. Earth Sci. 96, 60–67.
Marques, R., Waerenborgh, J.C., Prudêncio, M.I., Dias, M.I., Rocha, F., Ferreira da Silva, E., 2014b. Iron speciation in volcanic topsoils from Fogo island (Cape Verde) – iron oxide nanoparticles and trace elements concentrations. Catena 113, 95–106.
Marques, R., Prudêncio, M.I., Waerenborgh, J.C., Rocha, F., Ferreira da Silva, E., Dias, M.I., Madeira, J., Vieira, B.J.C., Marques, J.G., 2016. Geochemical fingerprints in topsoils of the volcanic Brava Island, Cape Verde. Catena 147, 522–535.
Marques, R., Prudêncio, M.I., Waerenborgh, J.C., Rocha, F., Ferreira da Silva, E., Dias, M.I., Vieira, B.J.C., Marques, J.G., Franco, D., 2017. Volcanic Conduits of the Chã das Caldeiras caldera (Fogo Island, Cape Verde) – REE and Fe crystalchemistry. WRI-15. P. Earth Pt. Sci. 17, 928–931.
Martinho, M.A., Gouveia, M.A., Prudêncio, M.I., Reis, M.F., Cabral, J.M.P., 1991. Factor for correcting the ruthenium interference in instrumental neutron activation analysis of barium in uraniferous samples. Appl. Radiat. Isot. 42, 1067–1071.
Mata, J., Munhá, J., Kerrich, R., 1999. Evidências para a ocorrência de metassomatismo carbonatítico na fonte mantélica da Ilha da Madeira. Anais V Cong. Geoq. PLP. 550–551.
Mata, J., Moreira, M., Doucelance, R., Ader, M., Silva, L.C., 2010. Noble gas and carbon isotopic signatures of Cape Verde oceanic carbonatites: implications for carbon provenance. Earth Planet. Sci. Lett. 291 (1–4), 70–83.
Mattielli, N., Weis, D., Blichert-Toft, J., Albarède, F., 2002. Hf istope evidence for a Miocene change in the Kerguelen mantle plume composition. J. Petrol. 43 (7), 1327–1339.
Miravet, R., López-Sánchez, J.F., Rubio, R., Smichowski, P., Polla, G., 2007. Speciation analysis of antimony in extracts of size-classified volcanic ash by HPLC-ICP-MS. Anal. Bioanal. Chem. 387, 1954–1979.
Möller, P., 1998. Rare Earth Elements and Yttrium Fractionation Caused by Fluid Migration. In: Novak, M., Rosenbaun, J. (Eds.), Challenges to Chemical Geology. Czech Geol Surv., Prague, pp. 9–32.
Moore, D.M., Reynolds, R.C., 1997. X-ray Diffraction and the Identification and Analysis of Clay Minerals, second ed. Oxford University Press.
Mourão, C., Mata, J., Doucelance, R., Madeira, J., Brum da Silveira, A., Silva, L.C., Moreira, M., 2010. Quaternary extrusive calcio-carbonatite volcanism in Brava Island (Cape Verde): a nephelinite–carbonatite immiscibility product. J. Afr. Earth Sci. 56 (2/3), 59–74.
Mourão, C., Moreira, M., Mata, J., Raquin, A., Madeira, J., 2012a. Primary and secondary processes constraining the noble gas isotopic signatures of carbonatites and silicate rocks from Brava Island: evidence for a lower mantle origin of the Cape Verde plume. Contrib. Mineral. Petrol. 163 (6), 995–1009.
Mourão, C., Mata, J., Doucelance, R., Madeira, J., Millet, M.-A., Moreira, M., 2012b. Geochemical temporal evolution of Brava Island magmatism: constraints on the variability of Cape Verde mantle sources and on carbonatite-silicate magmas link. Chem. Geol. 334, 44–61.
Murad, E., 1998. Clays and clay minerals: what can Mössbauer spectroscopy do to help understand them? Hyperf. Interact. 117, 39–70.
Peterson, A.L., Wolff, J.A., Tuberville, B.N., 1989. Eruption mechanisms of extrusive carbonatites on an ocean island: Brava, Cape Verde islands. EOS Trans. Am. Geophys. Union 70, 1421.
Prudêncio, M.I., Gouveia, M.A., Cabral, J.M.P., 1986. Instrumental neutron activation analysis of two French geochemical reference samples – basalt BR and biotite Mica-Fe. Geostand. Newslett. 29–31.
Prudêncio, M.I., Gouveia, M.A., Sequeira Braga, M.A., 1995. REE distribution in present-day and ancient surface environments of basaltic rocks (central Portugal). Clay Miner. 30, 239–248.
Prudêncio, M.I., Oliveira, F., Dias, M.I., Sequeira Braga, M.A., Delgado, M., Martins, M., 2006. Raw materials identification used for the manufacture of roman “Bracarense” ceramics from NW Iberian peninsula. Clay Clay Miner. 54, 639–651.
Prudêncio, M.I., Dias, M.I., Ruiz, F., Waerenborgh, J.C., Duplay, J., Marques, R., Franco, D., Ben Ahmed, R., Gouveia, M.A., Abad, M., 2010. Soils in the semi-arid area of the El Melah Lagoon (NE Tunisia) – variability associated with a closing evolution. Catena 80, 9–22.
Prudêncio, M.I., Dias, M.I., Waerenborgh, J.C., Ruiz, F., Trindade, M.J., Abad, M., Marques, R., Gouveia, M.A., 2011. Rare earth and other trace and major elemental distribution in a pedogenic calcrete profile (Slimene, NE Tunisia). Catena 87, 147–156.
Reimann, C., Matschullat, J., Birke, M., Salminen, R., 2010. Antimony in the environment: lessons from geochemical mapping. Appl. Geochem. 25, 175–198.
Silva, L., Le Bas, M.J., Robertson, A.H.F., 1981. An oceanic carbonatite volcano on Santiago, Cape Verde Islands. Nature 294, 644–645.
Stoppa, F., Pirajno, F., Schiazza, M., Vladykin, N.V., 2016. State of the art: Italian carbonatites and their potential for critical-metal deposits. Gondwana Res. 37, 152–171.
Thorez, J., 1976. Practical Identification of Clay Minerals. G. Lelotte, Dison, Belgium.
Traub, D.J., Gallup, B.V., Traub, M.A., Donald, T., 2009. Dental fluorosis in the Cape Verde Islands: prevalence of clinical findings in an isolated island population. Arch. Int. J. Med. 2 (2), 215–217.
Tuberville, B.N., Wolff, J.A., Le Bas, M.J., 1987. An oceanic nephelinite-phonolite-carbonatite association, Brava, Cape Verde islands. Eos 68, 1522.
Vandenberghe, R.E., De Grave, E., Landuydt, C., Bowen, L.H., 1990. Some aspects concerning the characterization of iron oxides and hydroxides in soils and clays. Hyperf. Interact. 53, 175–196.
Vandenberghe, R.E., Barrero, C.A., da Costa, G.M., Van San, E., De Grave, E., 2000. Mössbauer characterization of iron oxides and (oxy)hydroxides: the present state of the art. Hyperf. Interact. 126, 247–259.
Waerenborgh, J.C., Salamakha, P., Sologub, O., Gonçalves, A.P., Cardoso, C., Sério, S., Godinho, M., Almeida, M., 2000. Influence of thermal treatment and crystal growth on the final composition and magnetic properties of the YFe_xAl_{12-x} ($4 \leq - \leq 4.2$) intermetallics. Chem. Mater. 12, 1743–1749.
Woolley, A.R., Church, A.A., 2005. Extrusive carbonatites: a brief review. Lithos 85, 1–14.
Woolley, A.R., Kempe, D.R.C., 1989. Carbonatites: nomenclature, average chemical compositions, and element distribution. In: Bell, K. (Ed.), Carbonatites: Genesis and Evolution. Unwin Hyman, London, pp. 1–14.
Zhu, Y., An, F., Tan, J., 2011. Geochemistry of hydrothermal gold deposits: a review. Geosci. Front. 2 (3), 367–374.